

This article was downloaded by:

On: 22 January 2011

Access details: *Access Details: Free Access*

Publisher *Taylor & Francis*

Informa Ltd Registered in England and Wales Registered Number: 1072954 Registered office: Mortimer House, 37-41 Mortimer Street, London W1T 3JH, UK



The Journal of Adhesion

Publication details, including instructions for authors and subscription information:

<http://www.informaworld.com/smpp/title~content=t713453635>

Effect of Surface Topography on the Relaxation Behavior of Thin Polysulfone Coatings on Pretreated Aluminum Substrates

C. U. Ko^a; E. Balcells^a; T. C. Ward^a; J. P. Wightman^a

^a Center for Adhesive and Sealant Science, Virginia Polytechnic Institute and State University, Blacksburg, VA, U.S.A.

To cite this Article Ko, C. U. , Balcells, E. , Ward, T. C. and Wightman, J. P.(1989) 'Effect of Surface Topography on the Relaxation Behavior of Thin Polysulfone Coatings on Pretreated Aluminum Substrates', *The Journal of Adhesion*, 28: 4, 247 – 260

To link to this Article: DOI: 10.1080/00218468908030173

URL: <http://dx.doi.org/10.1080/00218468908030173>

PLEASE SCROLL DOWN FOR ARTICLE

Full terms and conditions of use: <http://www.informaworld.com/terms-and-conditions-of-access.pdf>

This article may be used for research, teaching and private study purposes. Any substantial or systematic reproduction, re-distribution, re-selling, loan or sub-licensing, systematic supply or distribution in any form to anyone is expressly forbidden.

The publisher does not give any warranty express or implied or make any representation that the contents will be complete or accurate or up to date. The accuracy of any instructions, formulae and drug doses should be independently verified with primary sources. The publisher shall not be liable for any loss, actions, claims, proceedings, demand or costs or damages whatsoever or howsoever caused arising directly or indirectly in connection with or arising out of the use of this material.

Effect of Surface Topography on the Relaxation Behavior of Thin Polysulfone Coatings on Pretreated Aluminum Substrates

C. U. KO, E. BALCELLS, T. C. WARD, and J. P. WIGHTMAN

Center for Adhesive and Sealant Science, Virginia Polytechnic Institute and State University, Blacksburg, VA 24061-0212, U.S.A.

(Received September 6, 1988; in final form February 2, 1989)

Thin polysulfone (PSF) coatings on pretreated aluminum surfaces were characterized utilizing dielectric thermal analysis (DETA) to detect changes in the molecular motions and structural transitions in the PSF-Al interphase. The XPS results show that the interfacial chemistry between the PSF and the Al oxide surface was the same on both degreased and phosphoric acid anodized (PAA) Al surfaces. The order of the loss peak temperature of the PSF is, PSF coating on porous Al > PSF coating on smooth Al > neat PSF film. The activation energy of relaxation is also lower for neat PSF when compared with the thin film cast onto a smooth Al or a porous PAA Al substrate. The SEM photomicrographs revealed that the PSF uniformly coated the degreased substrate, whereas PSF filled the porous oxide on PAA Al surface and resulted in whisker-like structures.

KEY WORDS Polysulfone coating; metal/polymer interphase; surface topography; whisker-like structure; interphase chemistry; viscoelastic behavior of coatings.

I INTRODUCTION

In describing the interactions between an adhesive and an adherend, it may not be sufficient to consider only the bulk properties of the materials involved. Thus, Sharpe,¹ among others, has used the concept of a three-dimensional “interphase” to describe this zone between bulk adhesive and bulk adherend. This zone extends from some point in the adherend where the local properties begin to change from the bulk properties, through the interface, and into the adhesive where the local properties again approach those of the bulk. In addition, this interphase region is postulated to extend from a few nanometers to a few thousand nanometers depending on the adhesive-adherend system. This paper focuses on the metal/polymer interphase.

There has been extensive research done to understand polymer-metal adhesion.^{2–6} It is known that various factors are involved in polymer-metal

adhesion including the physical and chemical nature of the metal surface,^{7,8} the existence of a weak boundary layer,⁹ toughening mechanisms as well as internal stresses of the adhesive.¹⁰ Other authors have noted that a gradient in material properties exists in such an interphase and for certain systems this can extend out to 0.2 mm from the metal surface.¹¹ Although the extent of polymer-filler interphase region was discussed,^{12,13} the influence of surface topography on the viscoelastic properties of the interphase region was not studied.

Indeed, there is conflicting evidence on the influence of a rigid substrate or filler on the small-strain viscoelastic properties of a thin bond line. Recent modeling has predicted a shift in the relaxation maxima of $\tan \delta$ curves which was attributed to changes in boundary layer properties of the polymer molecules.¹⁴ Such modeling involves the application of a three-phase system, effectively a composite, for predicting conditions for the shift and resolution of relaxation maxima of $\tan \delta$ curves. The three phases are the boundary-layer polymer, the bulk polymer, and the filler. Calculation of the glass transition temperature of filled polymers follows from two assumptions. First, the boundary layer, having properties differing from the bulk polymer due to the action of the filler surface, and the bulk polymer have different glass transition temperatures. Second, the filler, whose concentration determines the concentration ratio of boundary layer polymer to bulk polymer, also affects the shape of $\tan \delta$ curves because of its high modulus.¹⁴ Experimental work by Lipatov *et al.*¹⁵ showed that the addition of glass beads into epoxy resin resulted in a shift in the glass transition temperature to higher temperatures and a decrease in the maxima values of $\tan \delta$. Similar results were observed for epoxy resins filled with quartz powder. For poly(butyl methacrylate) filled with glass beads there was a considerable decrease and some broadening of the relaxation maxima. However, there was no shift in the glass transition temperature for this latter system. Their results were explained in terms of a decreased molecular mobility of the boundary-layer polymer due to the effect of the filler.

The idea of an "interphase" of polymer with modified properties has frequently been referred to in reports on filler or substrate modification of polymer response near T_g 's.¹⁶ However, there is comment in the literature which seriously questions the ability of a high modulus surface to influence macromolecules at any significant distance from the interface.¹⁷ Indeed, it is clear that because of the high possibility of residual stress fields due to thermal or curing operations in the preparation of filled or bonded polymer systems it may be quite difficult to identify mechanistically the origin of any anomalous behavior. Nevertheless, mathematical modeling of the interphase to allow for increases or decreases in the T_g of a filled composite has now appeared.¹⁸ Theocaris and Spathis predict that strong bonding between a filler and its matrix material results in a higher composite T_g , weak bonding leading in the opposite direction.¹⁸

In order to gain further insight into the fundamentals of adhesion, the properties of thin thermoplastic polysulfone films (PSF) on an aluminum substrate were chosen for this investigation. The interaction of the aluminum oxide layer with polysulfone was characterized with XPS (X-ray photoelectron

spectroscopy) in order to monitor the energy shift of the core electrons for differently pretreated surfaces. Scanning electron microscopy was used to study the aluminum surface topography for two different pretreatments and to measure the film thickness of the coated PSF films. In addition, thin polysulfone films coated onto a smooth and a porous surface were compared with respect to their dielectric relaxation behavior by dielectric thermal analysis.

II EXPERIMENTAL

A Sample preparation

1 *Polymer sample* Udel P-1700 polysulfone (General Electric) with a number average molecular weight of 26,000 g/mol and a polydispersity of 2.10 was used as the thermoplastic adhesive resin.¹⁹ A neat film of 260 μm in thickness was prepared by compression molding at 290°C followed by thermal treatment at 220°C for 1 hour in order to eliminate internal stresses due to pressing.

2 *Polymer coated samples* The coating substrate was an aluminum foil which was pretreated by vapor degreasing in one case and by phosphoric acid anodization (PAA) in another. It was thought that the degreasing pretreatment would result in a smooth surface whereas the PAA treatment would result in a porous surface; this was supported by HSEM (high resolution scanning electron microscopy) results as discussed below. Vapor degreasing was done with 1,1,1 trichloroethane for 30 minutes. The procedure for phosphoric acid anodization has been described.²⁰ The samples were anodized in a 10% phosphoric acid solution for 20 minutes with a current density of 6.5 mA/cm² at room temperature. The apparatus used for anodization was a potentiostat/galvanostat (Model 173 EG&G/Princeton Applied Research), and an electrometer (Model 178 EG&G/Princeton Applied Research) to provide constant current for the anodization. Thin film coatings were prepared from solutions in chloroform by spin coating. Samples were annealed 1 hour at 200°C prior to analysis in order to avoid results characteristic of the sample preparation.

B Characterization of substrate surface topography by high resolution scanning electron microscopy (HSEM)

HSEM photomicrographs were obtained on a Phillips EM-420T electron microscope. Thin Al samples were used and coated with Pd-Pt about 2 nm thick. Properly deposited, this layer does not alter the surface topography within the resolution of the microscope.

C Characterization of polysulfone coated systems

1 *X-ray photoelectron spectroscopy (XPS)* XPS studies were done using a Physical Electronics ESCA 5300 electron spectrometer with a magnesium anode

(1.254 keV). All samples were punched as 1.0 cm disks and scanned from 0 to 1100 eV. Major photopeaks were scanned repetitively to obtain the atomic fraction of elements on the sample surface. The coated PSF as well as the neat film surfaces were characterized with XPS. An argon ion beam was used for depth profiling in order to study the chemical composition of the interphase. Ion sputtering was done at a 40° angle to the sample with 3 kV energy beam of argon ions having a beam current of 30 μ A for successive periods of 5 minutes. The sputtering was continued until both the Al 2*p* and S 2*p* photopeaks were detected.

2 Scanning electron microscopy (SEM) The aluminum substrate was flooded with the 6 and 10 wt.% PSF in chloroform solution and spun at 500–4000 RPM. Different film thickness can be obtained by varying the solution concentration and the spincoater speed. The PSF coatings were fractured in liquid nitrogen after removing the Al substrate in 5% NaOH solution. The thickness of the resulting fractured film was measured using an ISI-SX-40 scanning electron microscope. Fractured surfaces were sputter coated with gold using an Edwards S150 B sputter coater.

3 Dielectric thermal analysis (DETA) The dielectric loss factor, $\tan \delta$, was followed as a function of both temperature and frequency with a Polymer Laboratory Dielectric Thermal Analyzer. The dielectric bridge allows the measurement of $\tan \delta$ at various preset frequencies with a variable applied field ranging from 5 mV to 1.275 V. All samples were analyzed with an applied field of 0.1 volt and scanned at 4 deg/min. from 160 to 250°C with a multifrequency (0.1–100 kHz) analysis routine. The coated sample (33 mm in diameter) was sandwiched between two stainless steel electrodes which had been covered with aluminum foil. In order to insure good contact between the electrode and foil, contact pressure was adjusted by a spring lock system.

III RESULTS AND DISCUSSION

A Surface topography after surface pretreatment

The degreased aluminum surface was studied with HSEM in order to determine the surface topography. The resulting HSEM photomicrograph in Figure 1a at 25,000 \times magnification revealed that pretreatment of the aluminum surface by vapor degreasing results in a relatively smooth surface showing only some machine rolling marks. Phosphoric acid anodization on the other hand resulted in a porous surface topography. Figure 1b at 50,000 \times magnification shows the fully developed porous oxide layer with pore diameters of approximately 100 nm.

B Interphase chemistry of the PSF—aluminum oxide by XPS

In Figure 2, both the O 1*s* and S 2*p* photopeaks are shown for the different samples. The binding energies (B.E.) in eV for each observed photopeak are

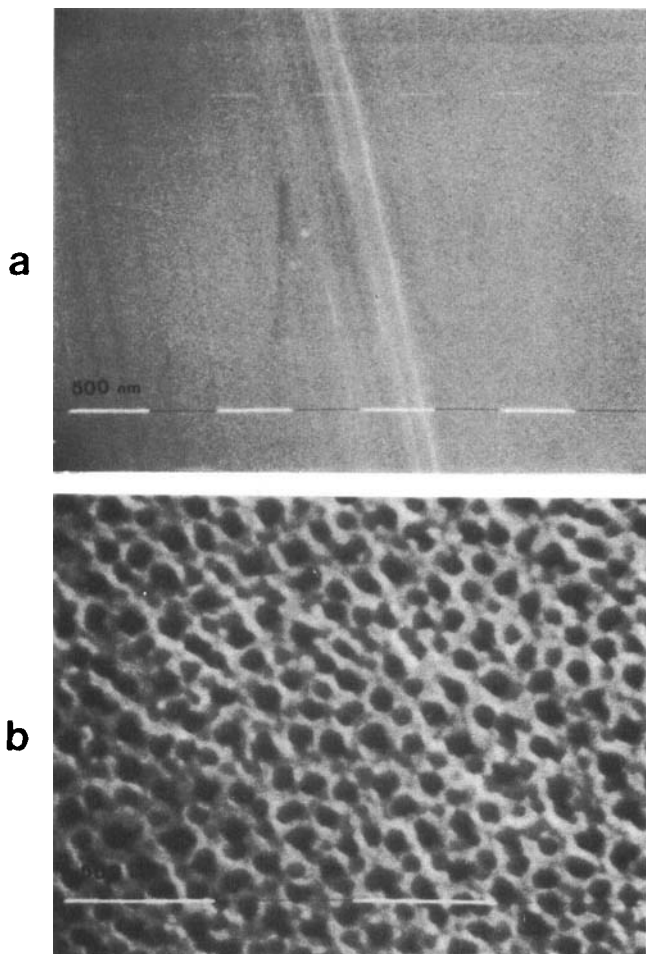


FIGURE 1 HSEM photomicrograph of a) aluminum surface pretreated by vapor degreasing (25,000 \times), b) aluminum surface pretreated by phosphoric acid anodization (50,000 \times).

tabulated along with the calculated values of the atomic fractions (A.F.) in Table I.

1 Neat PSF film The O 1s photopeak shows a doublet (Figure 2-I a), where one peak at 533.2 eV is associated with the $S = 0$ in the PSF, and the other peak at 531.9 eV is associated with the $-\phi - O$ group in PSF. The binding energy of the sulfur is 167.8 eV with an atomic fraction of 0.025 (Figure 2-I b).

The neat PSF film was argon ion beam sputtered and subsequently analyzed by XPS in order to determine any changes induced in the film by the ion sputtering process. It is shown in Figure 2-I d that the binding energy of the sulfur 2p photopeak is shifted to 163.8 eV from 167.8 eV (see Figure 2-I b) as evidence of

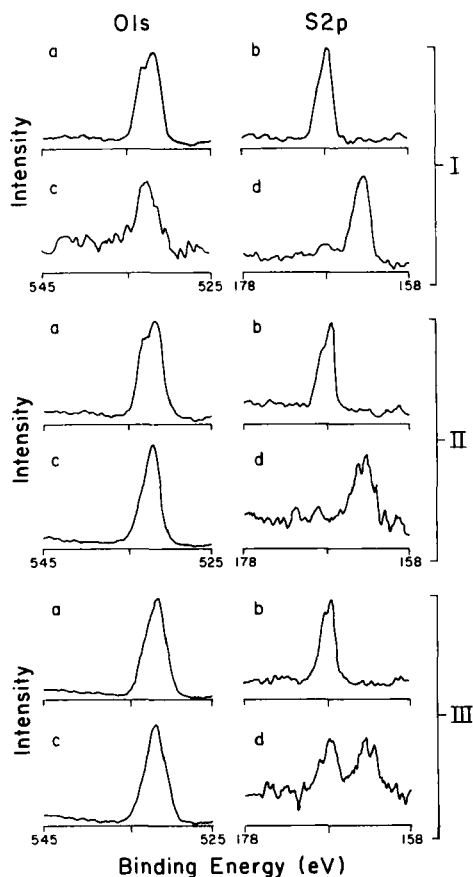


FIGURE 2 XPS results of O 1s and S 2p photopeaks: I. a, b) neat polysulfone film, c, d) after argon ion beam sputtering; II. a, b) PSF coating on degreased Al, c, d) after argon ion beam sputtering; III. a, b) PSF coating on PAA Al, c, d) after argon ion beam sputtering.

decomposition of PSF by argon ion beam bombardment. The intensity of the O 1s photopeak is also reduced by argon ion beam bombardment (see Figure 2-I c).

2 PSF coating on degreased Al surface XPS results before argon ion beam sputtering are shown in Figure 2-II a,b. The degreased Al sample coated with a 10 nm thick PSF film showed an O 1s doublet photopeak with binding energies at 533.2 and 531.8 eV similar to the neat PSF film. Indeed, the binding energy as well as the atomic percentage of the S 2p peaks are both similar to the values for the neat PSF film.

When the above sample was sputtered with an argon ion beam, the atomic percentage of aluminum in the sputtered surface increased, indicating that XPS was probing the PSF-Al interphase region. Also, the oxygen peak was now a single peak (Figure 2-II c) and the binding energy of the S 2p peak was again

TABLE I
XPS results of a neat polysulfone film, polysulfone coating on degreased aluminum, and polysulfone coating on PAA aluminum before and after argon ion beam sputter

Photopeak	PSF Film			
	Before Ar ion sputter		After Ar ion sputter	
	B.E. (eV)	A.F.	B.E. (eV)	A.F.
C 1s	284.6	0.79	284.6	0.94
O 1s	533.2	0.18	532.5	0.04
S 2p	531.9 167.8	0.025	163.8	0.02
PSF coating on degreased Al				
C 1s	284.6	0.72	284.6	0.52
O 1s	533.2	0.21	532.2	0.27
Al 2p	531.8 74.4	0.04	75.4	0.19
S 2p	167.7	0.028	163.3	0.013
PSF coating on PAA Al				
C 1s	284.6	0.56	284.6	0.40
O 1s	531.7	0.31	532.0	0.40
Al 2p	74.5	0.11	74.7	0.18
S 2p	167.6	0.02	167.9 163.6	0.01
P 2p	134.6	0.01	134.9	0.01

shifted from 167.8 to 163.3 eV (Figure 2-II d), which resembles the results for a sputtered neat film.

3 PSF coating on PAA surface A 50 nm PSF coating on a PAA Al surface was analyzed by XPS. The thicker film had to be applied in order to cover the entire porous oxide layer. Prior to sputtering, the aluminum 2p photopeak assigned to the aluminum oxide was present at 74.5 eV, and the sulfur peak at 167.6 eV was present with atomic fraction of 0.02. The P 2p photopeak at 134.6 eV on this surface was from the phosphoric acid used in the pretreatment.

When the sample was sputtered with an argon beam, the XPS results were quite different from those for the smooth surface. The sulfur 2p peak now had two separate peaks, one at 167.9 eV and the other at 163.6 eV (Figure 2-III d). It seems as though the polysulfone film from the top of the pores was changed (S 2p peak from 167.6 to 163.6 eV, Figure 2-III d) when ion sputtered. However, the peak at 167.9 eV may be due to polysulfone within the porous oxide which was not affected by the sputtering process. Hence, it appears that XPS was probing a part of the surface, namely the pores, which is not affected by ion beam sputtering. These results indicate that the interfacial chemistry between the PSF-Al oxide was the same for both the degreased and the PAA aluminum surfaces. However, in the PAA case the polysulfone molecules had penetrated

into the oxide pores which is clearly seen in the SEM photomicrographs. This is discussed in the next section.

C SEM of coated films

In Figure 3a, the film thickness of the PSF coating on the degreased Al substrate is shown to be about $2.0\ \mu\text{m}$ for one of the samples studied. Using the same

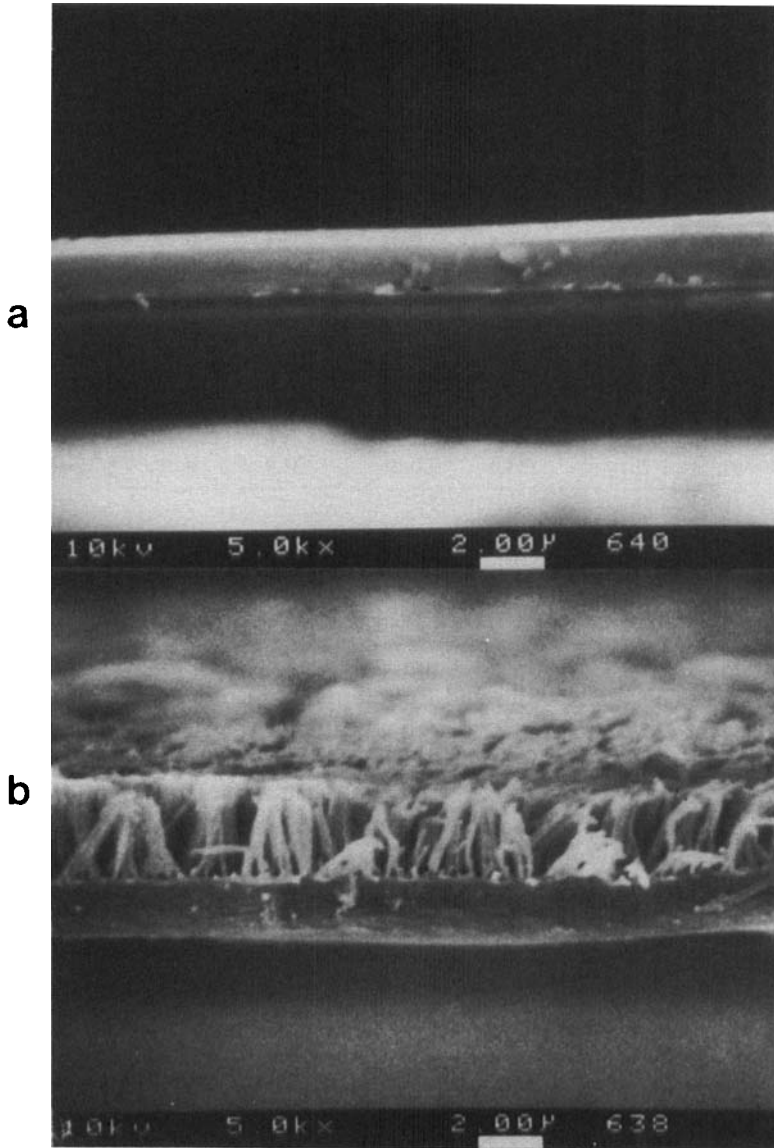


FIGURE 3 SEM photomicrographs ($5000\times$) for a $2.0\ \mu\text{m}$ PSF film coated on: a) degreased Al surface and b) PAA-Al surface.

concentration of PSF and spin coater speed, the resulting total film thickness of PSF on the PAA Al was about $4.2\ \mu\text{m}$, which includes an overlayer thickness of $2.0\ \mu\text{m}$ and a whisker layer thickness of about $2.2\ \mu\text{m}$ as shown in Figure 3b. The whiskers were the result of penetration of the PSF into the porous aluminum oxide. They had an average diameter of about $100\ \text{nm}$ which matched the pore diameter of the aluminum oxide. The penetration of the PSF ($2.2\ \mu\text{m}$ whiskers) was observed to occur for all films coated onto the PAA Al surface. This was observed even at a film thickness of $0.2\ \mu\text{m}$ as shown in Figure 4.

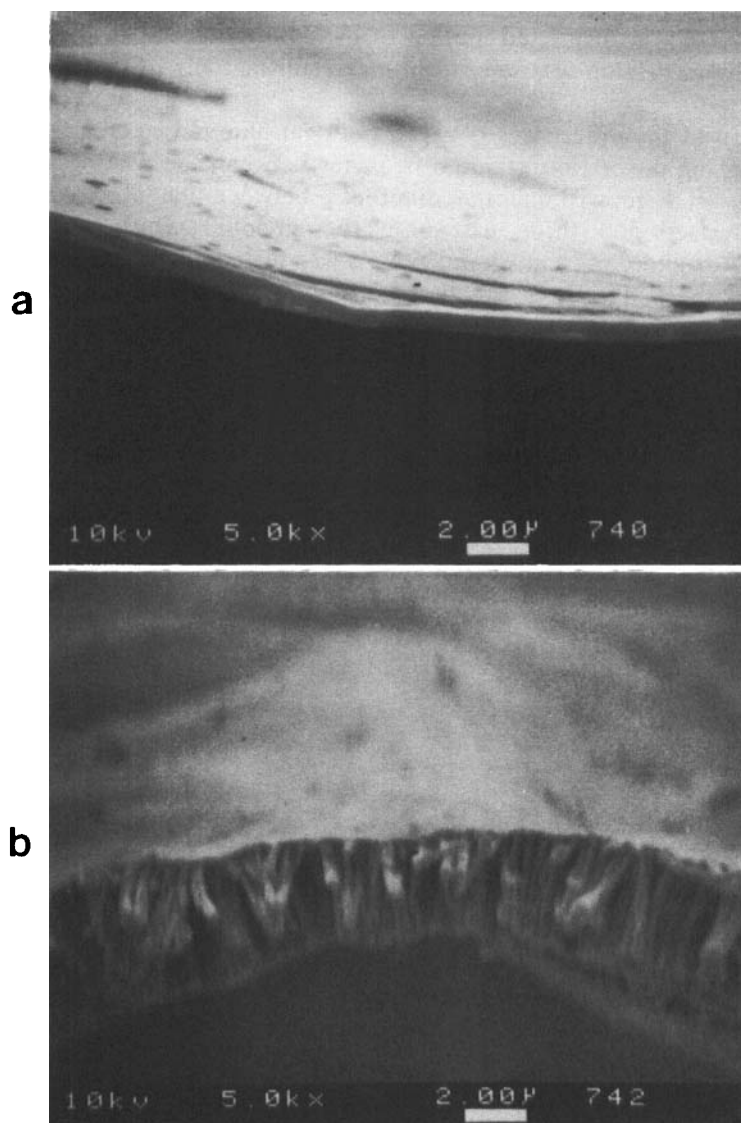


FIGURE 4 SEM photomicrographs ($5000\times$) for a $0.2\ \mu\text{m}$ PSF film coated on: a) degreased Al surface and b) PAA-Al surface.

D DETA results

Glass transition temperatures for the coatings and the neat films were determined from the peak maxima of the $\tan \delta$ versus temperature curves at frequencies in the range of 0.1 to 100 kHz. In Figure 5, the dielectric loss factor, $\tan \delta$, is plotted against temperature for both the neat PSF film and the PSF coatings shown in Figure 3. The coatings showed a response which was different from that of the neat film, both in the magnitude of the $\tan \delta$ values and the glass transition temperatures. While the decrease in the magnitude of the $\tan \delta$ for the coatings is due to the smaller sample size, the increase in the glass transition temperature is thought to be due to restricted motion of the PSF molecules in the case of the coatings. The dispersion was seen to broaden substantially in the case of coated PSF.

In addition to the differences between the neat film and coatings, there was a difference in the dielectric relaxation behavior between the coatings themselves. One notices in Figure 3 that the difference between the films cast onto the PAA Al surface and those cast onto the smooth surface resided in the whisker-like structure present when PAA Al was the coating substrate. Yet, from the dielectric thermal analysis, the glass transition temperature was always highest for the coatings on the PAA Al surface, with the magnitudes of $\tan \delta$ always lower for the films on the PAA Al surface and the breadth of the glass transition always greatest for the coatings on the PAA Al surface.

The lower values of $\tan \delta$ at the T_g , $\tan \delta_{T_g}$, for the coatings on the PAA-Al surfaces were interesting because one would expect higher $\tan \delta_{T_g}$ values for the films on the PAA-Al surface compared with the films on the degreased-aluminum surface. This is because the magnitude of $\tan \delta$ increases as the volume fraction of

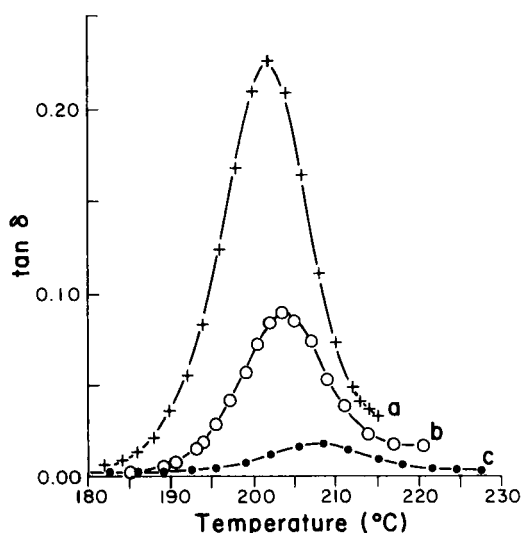


FIGURE 5 $\tan \delta$ versus temperatures for: a) neat polysulfone film, b) PSF coating on degreased Al surface shown in Figure 3a, c) PSF coating on PAA-Al surface shown in Figure 3b.

the relaxing phase increases.²¹ From Figure 3 the volume fraction of PSF was greater for the film on the PAA-Al surface due to the added whisker layer. However, the lower values of $\tan \delta_{T_g}$ for the films on the PAA Al surface, compared with those on the smooth aluminum surface, could be interpreted as resulting from higher interfacial shear strengths which themselves result from restricted segmental and molecular mobility of the polysulfone. This is consistent with work done by Chua who reported an inverse relation between $\tan \delta_{T_g}$ and the interfacial shear stress for glass fiber reinforced polyester systems.²² The authors feel that "intimate" contact of polymer with both the smooth and the anodized surfaces was achieved (no bubbles or pinholes) due to the dilute solution spin-coating method of application.

The glass transition temperatures and $\tan \delta_{T_g}$ values for the neat film and coatings of various thicknesses are given in Table II. In regard to the higher T_g values and the broader transitions for the films on the PAA aluminum surface, these differences in viscoelastic behavior can be attributed to the whisker-like structures present in the PSF/PAA Al system.

Arrhenius activation energies for relaxation were calculated from the frequency dependencies of the glass transition temperature. Figure 6 gives the calculated activation energy for PSF as a function of film thickness as determined from the SEM photomicrographs. The activation energy decreased as film thickness

TABLE II
Glass transition temperatures and $\tan \delta_{T_g}$ for neat PSF film, and coatings of various film thicknesses

Neat PSF Film					
T_g	Frequency (kHz)		$\tan \delta_{T_g}$		
202.0	1.0		0.23		
219.0	100.0		0.25		
PSF film on smooth Al					
1 kHz			50 kHz		
Film thickness (μm) ^a	T_g	$\tan \delta_{T_g}$	Film thickness (μm) ^a	T_g	$\tan \delta_{T_g}$
0.8	205.5	0.030	0.8	212.0	0.041
1.4	205.5	0.087	1.4	213.0	0.160
1.8	203.5	0.092	1.8	211.5	0.170
PSF film on porous-Al					
1 kHz			10 kHz		
Film Thickness (μm) ^a	T_g	$\tan \delta_{T_g}$	Film thickness (μm) ^a	T_g	$\tan \delta_{T_g}$
0.2	211.5	0.0097	0.2	225.5	0.012
2.0	209.0	0.017	2.0	221.5	0.024
5.0	210.0	0.034	5.0	223.5	0.060

^a Film thickness of the overlayer only.

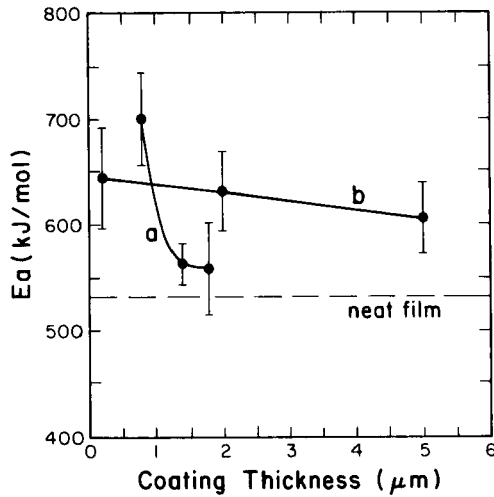


FIGURE 6 Arrhenius activation energy for PSF coatings as a function of overlayer film thickness only for: a) films cast onto a smooth aluminum surface; b) films cast onto a porous aluminum surface.

increased and approached that of the neat film (530 kJ/mol) at 1.4 μm for the PSF film on the smooth Al surface. For the PSF coating on the PAA Al surface, even at thickness of 2.0 μm , the activation energy was higher than that of the PSF film on degreased film at 1.8 μm . Since all samples were annealed prior to analysis, the differences in the Arrhenius activation energy with coating thickness suggest a gradient of relaxation properties in the interphase region. The higher activation energy for the thinner films would seem to indicate that, near the interface, the polymer properties were affected by the physical nature of the surface.

Referring to Figures 3 and 6, it is seen that the activation energy was approximately 100 kJ/mol higher for the PSF film coated onto the porous surface than on the smooth surface. Since the difference between the film coatings was the whisker-like structure present in the films deposited on the PAA-Al surface, it appears that the porous regions influenced the viscoelastic behavior of the PSF coatings by defining a restricted layer. These results were consistent with the differences in the glass transition temperatures and the $\tan \delta_{T_g}$ as reported above for the films shown in Figure 3. It is evident then that the surface topography can affect the T_g , $\tan \delta_{T_g}$, activation energy, and the breadth of the T_g of an adhesive in the interphase region.

IV CONCLUSIONS

The goal of this study was to correlate the observed dielectric relaxation results of thin PSF coatings with the chemical composition and topographical features of

the Al substrate. From this investigation, the following highlights were noted:

1. The degreased sample was a smooth surface whereas the PAA surface was a porous surface with a pore diameter of approximately 100 nm.
2. The XPS results show that the interfacial chemistry between the polysulfone and the aluminum oxide surface was the same on both degreased and PAA aluminum surfaces.
3. The SEM photomicrographs revealed that the PSF uniformly coated the degreased substrate, whereas PSF migrated into the porous oxide on PAA Al surface and resulted in whisker-like structures.
4. The magnitude of the dielectric loss factor was greatest for the neat film and lowest for the film on the PAA surface and the breadth of the glass transition was greatest for the PSF coating on the PAA Al surface.
5. The glass transition temperatures for the polysulfone was highest for the films on the porous aluminum surface where penetration had occurred.
6. The Arrhenius activation energy was seen to decrease with thickness and approach that of the neat film at about $1.4\ \mu\text{m}$ for the polysulfone film on a smooth degreased aluminum substrate. For the film on the PAA surface, the activation energy at $2.0\ \mu\text{m}$ was higher than that of the neat film.

V Acknowledgements

The authors acknowledge the financial support of the Alcoa Technical Center, the Adhesive and Sealant Council and the Center for Innovative Technology. We thank Frank Cromer for assistance in the SEM work. Enabling funds for the purchase of the surface analysis equipment came from the National Science Foundation and Virginia Tech.

References

1. L. H. Sharpe, in *Aspects of Adhesion*, D. J. Alner and K. W. Allen Eds., **7**, 139 (1973).
2. K. L. Mittal, *Pure and Appl. Chem.* **52**, 1295 (1980).
3. W. J. Van Ooij, *Surface Sci.* **89**, 165 (1979).
4. D. M. Brewis and D. Briggs, *Polymer* **22**, 7 (1981).
5. F. J. Boerio, C. A. Gosselin, R. G. Dillingham and H. W. Liu, *J. Adhesion* **13**, 159 (1981).
6. W. Brockmann, O. D. Hennemann and H. Kollek, *Intl. J. Adhesion and Adhesives* **1**, 33 (1982).
7. J. D. Venables, D. K. McNamara, J. M. Chen, T. S. Sun, and R. L. Hopping, *Appl. Surf. Sci.* **3**, 88 (1979).
8. D. E. Packham in *Adhesion Aspects of Polymeric Coatings*, K. L. Mittal Ed. (Plenum Press, N.Y., 1983), p. 19.
9. R. H. Hansen and H. Schonhorn, *J. Polymer Sci., part B* **4**, 203 (1966).
10. T. C. Ward, M. Sheridan, D. L. Kotzev, in *Adhesive Joints: Formation, Characteristics and Testing*, K. L. Mittal Ed. (Plenum Press, N.Y., 1983).
11. G. C. Knollman, *Intl. J. Adhesion and Adhesives* **5**, 137 (1985).
12. T. K. Kwei, *J. Polymer Sci., part A* **3**, 3229 (1965).
13. P. S. Theocaris, *J. Reinforced Plastics & Comp.* **3**, 204 (1984).
14. V. F. Babich and Y. S. Lipatov, *J. Appl. Polym. Sci.* **17**, 53 (1982).
15. Y. S. Lipatov, V. F. Rosovizky and V. V. Shifrin, *ibid.* **27**, 455 (1982).
16. G. J. Howard and R. A. Shanks, *J. Macromol. Sci.-Phys.* **B19**(2), 167 (1981).
17. P. Peyser, *Polym.-Plat. Technol. Engr.* **10**, 117 (1978).
18. P. S. Theocaris and G. D. Spathis, *J. Appl. Polym. Sci.* **27**, 3019 (1982).
19. M. J. Jurek, Ph.D. Dissertation, Virginia Polytechnic Institute and State University, Blacksburg, VA (1987).

20. Standard Practice for Preparation of Aluminum Surfaces for Structural Adhesive Bonding (phosphoric acid anodization) ASTM D 3933-80 (1980).
21. R. E. Wetton in *Dynamic Mechanical Analysis of Polymers and Related Systems*, J. V. Dawkins Ed. (Elsevier Applied Science Publishers, London, 1986).
22. P. W. Chua, *SAMPE Quarterly* **18**, 10 (1987).